

Fine-grained Text and Image Guided Point Cloud Completion with CLIP Model

Wei Song, Jun Zhou, Mingjie Wang, Hongchen Tan, Nannan Li, Xiuping Liu

Abstract—This paper focuses on the recently popular task of point cloud completion guided by multimodal information. Although existing methods have achieved excellent performance by fusing auxiliary images, there are still some deficiencies, including the poor generalization ability of the model and insufficient fine-grained semantic information for extracted features. In this work, we propose a novel multimodal fusion network for point cloud completion, which can simultaneously fuse visual and textual information to predict the semantic and geometric characteristics of incomplete shapes effectively. Specifically, to overcome the lack of prior information caused by the small-scale dataset, we employ a pre-trained vision-language model that is trained with a large amount of image-text pairs. Therefore, the textual and visual encoders of this large-scale model have stronger generalization ability. Then, we propose a multi-stage feature fusion strategy to fuse the textual and visual features into the backbone network progressively. Meanwhile, to further explore the effectiveness of fine-grained text descriptions for point cloud completion, we also build a text corpus with fine-grained descriptions, which can provide richer geometric details for 3D shapes. The rich text descriptions can be used for training and evaluating our network. Extensive quantitative and qualitative experiments demonstrate the superior performance of our method compared to state-of-the-art point cloud completion networks.

Index Terms—Multimodal fusion, text corpus, point cloud completion

INTRODUCTION

WITH the widespread use of 3D scanning devices such as LiDARs and RGB-D cameras, the acquisition of point clouds has become easier, which has promoted the development of a large number of research fields including automated machinery [1], driving autonomously [2], 3D visualization [3], scene understanding [4] and the production process [5]. However, due to factors such as occlusion, reflection, transparency, low resolutions that may exist in the actual scanning process, the obtained point clouds are generally scattered and incomplete. The incomplete point clouds can produce ambiguous and misleading information, making it more difficult to recognize and understand 3D shapes. This can severely limit the performance of some downstream tasks such as 3D point cloud reconstruction [6]–[8], detection and classification [9]–[14]. Therefore, the research of point cloud completion has attracted increasing attention from the 3D visual community in recent years.

Although deep neural network-based methods have achieved excellent performance in point cloud completion, the lack of geometric cues and the partial sparseness of the scanned point cloud have hindered the further development of 3D point cloud completion task. Compared with the scanned point clouds, images can provide superior resolution and richer textures. Meanwhile, cross-sensors such as depth cameras and camera-LiDAR scanners [15] are now available and less expensive to collect both colorful images and point clouds of 3D scenes, where images

can provide more complementary geometry and semantic cues. The effectiveness of the image modality information introduction has been verified in recent literatures [16]–[18]. However, the existing methods mainly rely on the multi-view images and point clouds provided by the ShapeNet-ViPC dataset, which is a small-scale dataset. Insufficient training data leads to poor generalization ability of the trained network, making it difficult for the network to predict missing semantic and geometric details of incomplete shapes.

Furthermore, humans are considered to stand out among the animal world for their special ability to use language to describe objects, environments and events. Language can not only describe the physical and functional properties of objects, but also distinguish subtle differences between these properties through rich modifiers. Recent advances in the fields of language modeling [19], [20], text-conditioned image generation [21]–[26] and text-conditioned 3D shape generation [27]–[34] have demonstrated the effectiveness of textual descriptions as an efficient and valuable source of information. Therefore, text descriptions, as another important modality information, must be able to characterize richer shape semantics for point cloud completion task. However, due to the lack of a dataset including enough pairs of texts and point clouds, there remains an unexplored area in investigating the use of text as auxiliary information for point cloud completion. Although Text2Shape [35] has exhibited promising results by curating a considerable dataset of natural language descriptions for various 3D objects, especially chairs and tables from the ShapeNet dataset [16]. Regrettably, given the associated costs, this approach is difficult to apply to constructing larger-scale and multi-category 3D object text dataset. Furthermore, the text descriptions generated by Text2Shape [35] cover multiple aspects of 3D objects, including color, texture and other shape details, but lacks sufficient geometric appearance information. As a result, this leads to redundant text descriptions that may exceed the input

W. Song, J. Zhou and N. Li are with the School of Information Science and Technology, Dalian Maritime University, Dalian, China (E-mail: songwei100110@gmail.com, zj.9004@gmail.com, nannanli@dlmu.edu.cn).

M. Wang is with the School of Science, Zhejiang Sci-Tech University, Zhe Jiang, China (E-mail: mingjiew@zstu.edu.cn).

H. Tan is with the Institute of Artificial Intelligence, Beijing University of Technology, Beijing, China (E-mail: tanhongchenphd@bjut.edu.cn).

X. Liu is with the School of Mathematical Sciences, Dalian University of Technology, Dalian 116024, China. (E-mail: xpLiu@dlut.edu.cn).

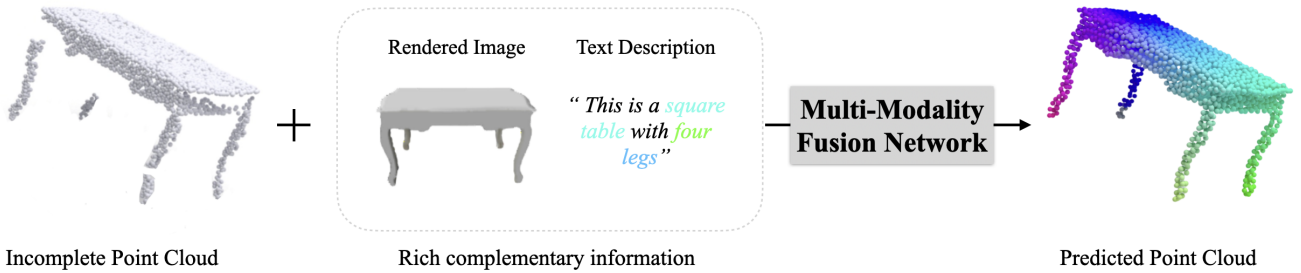


Fig. 1. This is a novel point cloud completion method that can predict reliable complete shapes by leveraging the rich complementary information from a corresponding rendered image and rich text descriptions.

capacity of the CLIP [36] text branch (77 tokens only), and more geometric details may be lost when extracting textual features.

In this paper, we propose a novel multimodal point cloud completion network that can simultaneously fuse the extra visual and textual information, as shown in Fig. 1. First, unlike the previous paradigm of multimodal point cloud completion for point-image pair fusion, we introduce additional text descriptions into the model to improve the model’s ability to perceive shape semantics. Then, considering the relatively small scale of training data in the previous multimodal point cloud completion methods [16]–[18], this leads to insufficient training of the extra modality branch. Therefore, inspired by the works [36]–[39], which introduce pre-trained models on large-scale dataset and demonstrate great generalization to a wide range of tasks, we transfer the pre-trained multimodal knowledge including visual and textual modalities from CLIP to our point cloud completion network. Compared with the scale of about 608k trained samples in the ShapeNet-ViPC dataset [16], the pre-trained CLIP model uses about 400 million training samples, ensuring that more effective textual and visual features can be extracted. Moreover, to address the limited scale and redundancy issues encountered with Text2Shape, and to mitigate the lack of text descriptions for 3D shapes in ShapeNet-ViPC [16], we introduce the ViPC-Text dataset. This dedicated dataset focuses on capturing descriptive information concerning geometric parts within 3D shapes. It is worth noting that we propose an innovative approach for generating large-scale and compact text descriptions, thereby facilitating the generation of text descriptions for arbitrary 3D shapes.

In summary, the contributions of this study are threefold:

- Considering the generalization and reliability of large models, a pre-trained model is employed to effectively transfer multimodal features extracted from images and texts into our multimodal completion framework.
- A large-scale fine-grained corpus of 3D shapes named ViPC-Text is introduced to further explore the complementarity of text descriptions of 3D geometry with the missing semantics and structure of incomplete shapes. Furthermore, the method for generating 3D text descriptions can also be flexibly extended to arbitrary 3D shapes.
- A novel point cloud completion network is designed to simultaneously use three modality information including point clouds, images and texts. Extensive experiments demonstrate the superior performance of our method against previous state-of-the-art methods.

2 RELATED WORK

In recent years, stimulated by the great success of deep learning [40] in various vision tasks [41], the learning-based paradigms have become the dominant direction in the realm of point cloud completion [42] and has achieved outstanding performance. Existing learning-based point cloud completion can be classified into two types: unimodal and multimodal methods. In this section, we review these two types of methods in detail. Furthermore, we briefly introduce CLIP technology, which is employed in our proposed network for multimodal feature extraction.

2.1 Unimodal Point Cloud Completion

Unimodal point cloud completion only relies on information from a given incomplete point cloud to predict the missing part. Among them, PCN [43] is a pioneering work that directly operates on incomplete point clouds by using a point cloud network for predicting complete shapes. Compared to traditional methods, the PCN [43] avoids the need for any prior assumptions regarding the shape’s structure such as symmetry, or requiring annotations related to the underlying shape such as category information. Besides, benefiting from the design of a folding-based encoder, this method is able to generate the missing details of the incomplete shapes while maintaining a relatively low number of parameters. Subsequently, TopNet [44] designs a hierarchical decoder with the root tree structure, which can progressively generate a series of sub-nodes containing structured point clouds. Thus, the subset of points contained in the child nodes can be pieced together to form a final complete shape. MSN [45] is also a coarse-to-fine completion method, which can predict complete shapes by assembling a collection of estimated surface elements. Recently, inspired by transformer technology [46] used in the visual tasks, the architectures of Point Transformer [47], [48] are proposed and widely used in the tasks of point cloud processing. Based on this technology, PointTr [49] represents the point clouds as a set of unordered groups of points with position embeddings and converts the point clouds to a sequence of proxies under the way of encoder-decoder. SnowflakeNet [50] utilizes a Skip-Transformer to generate child points by gradually splitting parent points and predicting the complete shapes with more details. Also using the transformer technology, some recent works [51]–[53] employ a coarse-to-fine approach based on proxy points for point cloud completion. Specifically, Seedformer [51] primarily utilizes seeded proxies to complete the point cloud through point upsampling layers. Then, ProxyFormer [53] divides the point clouds into existing and missing parts and facilitates communication

between the two parts using proxies. Besides, AnchorFormer [52] models regional discrimination by learning a set of anchors based on the point features of the input partial observation, which further employs a modulation scheme to transform a canonical 2D grid into a detailed 3D structure at specific locations of the sparse points. Although this kind of methods have achieved good performance, it is difficult for unimodal techniques to overcome the ambiguity of incomplete data itself, which makes it difficult for 3D completion methods to make greater breakthroughs.

2.2 Multimodal Point Cloud Completion

Multimodal completion task aims to utilize complementary modality information to improve the quality of the complete shapes, which is pioneered by ViPC [16]. The motivation for this method is that the extra modalities contain the necessary structure or semantic information of the missing part of a given shape. Particularly, ViPC [16] uses an image to predict the global shape information that is lacking in the incomplete point cloud. Then, the predicted coarse point cloud from the single-view image is used to guide the fine-grained completion. However, due to the lack of direct multimodal feature fusion at the coarse-grained stage, the use of complementary information in images is not sufficient. To solve this problem, XMFNet [17] proposes a multimodal feature fusion network to effectively combine features extracted from the two modalities in a localized latent space, thus avoiding the hard inverse problem of directly reconstructing point clouds from images. Moreover, CSDN [18] proposes a cross-modal shape-transfer dual-refinement network, so that the auxiliary image can participate in the coarse-to-fine completion pipeline in the whole cycle. The guidance of multimodal information can significantly improve the quality of complete shapes, and our proposed method also adopts the paradigm of multimodal fusion. But unlike the methods mentioned above, we introduce a pre-trained large model to greatly increase the number of samples, which ensures that the multimodal complementary information can be effectively extracted. In addition, we expand the category of multimodal information by adding text descriptions to further increase complementary semantic information. Last but not least, a corpus with rich fine-grained geometric information is also proposed, and the text descriptions can effectively improve the semantic and geometric structure prediction capabilities of multimodal networks for incomplete shapes.

2.3 CLIP-based 3D Task

Recently, CLIP [36] represents a noteworthy advancement in training visual models by natural language supervision, resulting in strong alignment between textual modal data and visual modal data. This alignment enables the models to uncover important feature information from novel perspectives that may be present in the other modality. Inspired by CLIP, CLIP-Based 3D point cloud analysis tasks have attracted increasing attention from the research community. For the 3D shape understanding task, PointCLIP [54] and PointCLIP V2 [55] convert 3D representation to multi-view image representation and attempt to process 3D information using CLIP [36], which can achieve knowledge transfer from 2D to 3D and conduct 3D recognition via CLIP pre-trained in 2D. However, these works do not directly use point cloud representation, resulting in insufficient geometric feature extraction. Differently, the current works [56]–[59] attempt to use natural language supervision to train the triplets including point clouds,

corresponding rendered 2D images, and text descriptions, thus directly obtaining the feature representation of the point cloud. Therefore, the 3D features extracted from this kind of method can achieve zero-shot capabilities, which are similar to the features extracted from CLIP. The above methods have demonstrated the generalization and strong representation ability of CLIP for 3D tasks. Inspired by this, we also propose a CLIP-based multimodal guided point cloud completion network.

3 METHOD

3.1 Overview

The goal of this paper is to explore the effectiveness of rich multimodal information for point cloud completion. The pipeline of our network is shown in Fig. 2. First, in order to take advantage of the generalization ability of the large model, we use the CLIP model to extract the features of multimodal information. Second, a multi-stage feature fusion strategy is used in our backbone network to achieve the effective fusion of multimodal information. Finally, we propose an efficient text generation algorithm and build a corpus with fine-grained geometric descriptions to further improve the model’s understanding of semantics and geometric structures. In Sec. 3.2, we first give an overview of our proposed multi-modality fusion network, which can achieve state-of-the-art performance. Then in Sec. 3.3, we briefly review the pre-trained visual and textual encoders employed in our network. Subsequently, We show the LLM-assisted 3D component corpus in Sec. 3.4. In Sec. 3.5, we describe the our proposed fusion strategy in detail. To the end, we show the loss function used for training and evaluating in Sec. 3.6.

3.2 Overview of Multi-modality Fusion Network

Inspired by XMFNet [17], we design a novel architecture for 3D point cloud completion, which adopts richer modality information and a multi-stage fusion strategy. Similar to XMFNet [17], the basic network consists of two modality-specific feature extractors to construct the fine-grained features for point clouds and images, and then an attention module is employed for feature fusion, as shown in the upper part of Fig. 2. Here, an incomplete point cloud $X_p \in \mathbb{R}^{N \times 3}$ and a randomly selected rendered images $X_i \in \mathbb{R}^{3 \times 224 \times 224}$ from 24 perspectives are fed into the network, then a complete point cloud $Y \in \mathbb{R}^{2048 \times 3}$ is predicted. Since this architecture only introduces the multimodal information from images and point clouds and only trains on a small-scale dataset, the semantic information acquired by this basic network is not sufficient and the generalization ability of this network is poor. To solve this problem, we introduce a pre-trained CLIP model [36] on top of this basic network to extract more powerful multimodal information from images and text descriptions, as shown in the bottom of Fig. 2. The pre-trained CLIP model has a more strong generalization ability and can obtain feature representations with more semantic information, which can help to improve the performance of the basic point cloud completion network. See the bottom of Fig. 2, the pre-trained CLIP [36] consists of textual and visual encoders, which can provide more comprehensive modal information to guide the completion process. Furthermore, to extract more information about the geometric features of the point cloud to improve the understanding of the point cloud, (see the bottom of Fig. 2), we generate fine-grained geometric text descriptions for the point cloud, which can be used to accurately

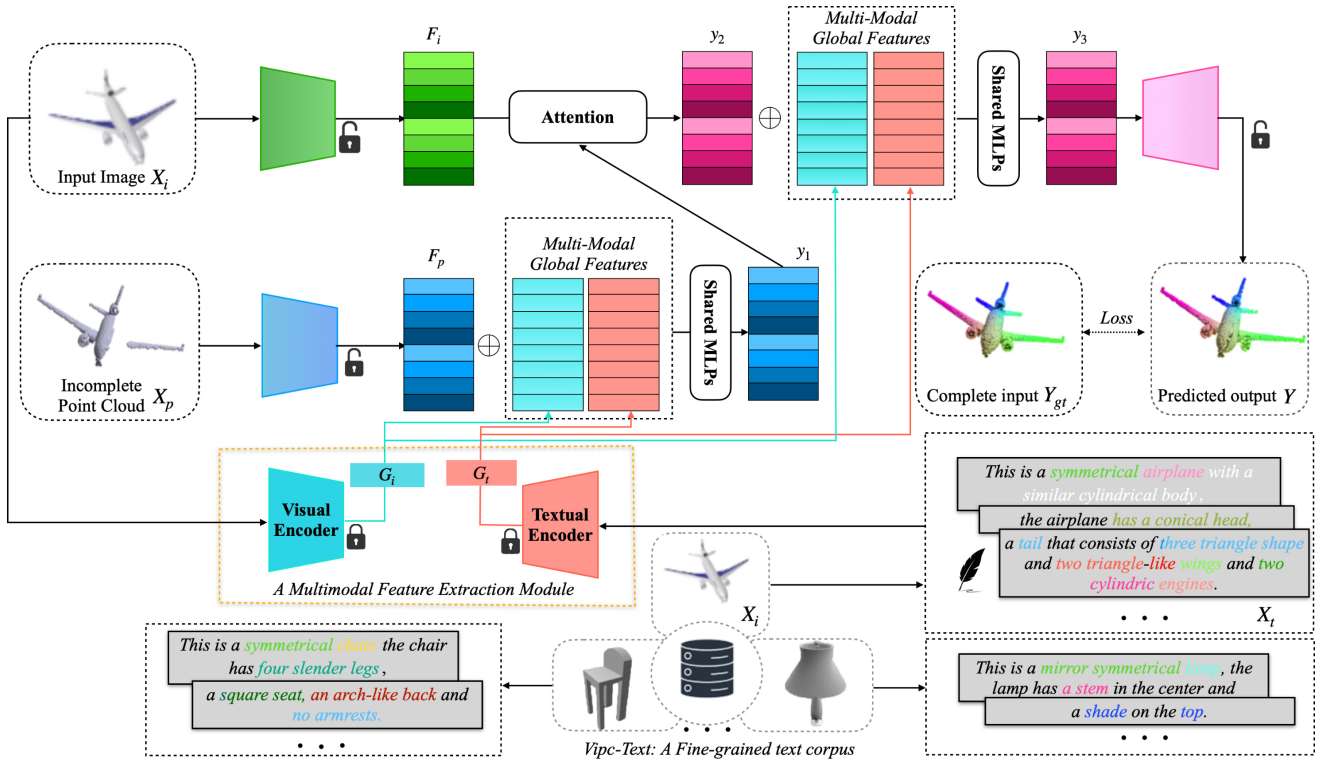


Fig. 2. Architecture of the proposed Fine-grained Text and Image Guided Point Cloud Completion using CLIP, see Sec. 3.1 in the text for more details.

locate the semantic parts of the point cloud and provide rich geometric structure information. Ultimately, the global geometry-aware features $G_i \in R^{512 \times 1}$ and $G_t \in R^{512 \times 1}$ are available from the visual encoder and textual encoder respectively. Notably, we design a multi-stage multimodal feature fusion mechanism to ensure that multimodal features with richer semantic and geometric representations can effectively guide the process of point cloud completion. In the following, we present each module of the proposed method in more detail.

3.3 Visual and Textual Encoders

CLIP [36] is a pre-trained model that includes a visual encoder and a textual encoder, which are learned by matching about 400 million image-text pairs. The scale of the training dataset ensures the generalization of the model and the alignment of multimodal features allows the two encoders to extract latent features with unified semantics and visual consistency, which are beneficial for the task of point cloud completion. In this study, we embed this pre-trained model into our completion architecture. First, rendered images derived from point clouds in the ShapeNet-ViPC dataset [16] are utilized as input to the visual encoder of CLIP. Simultaneously, the textual encoder can accept a specific textual prompt that includes a defined template: “This is a [category]” and the “category” word should correspond to the shape category in the ShapeNet-ViPC dataset [16]. Furthermore, a richer description such as “This is a classic styled, white and metal-based table” (replace with a better textual description containing structural information) can also follow the previous prompt as a semantic extension. The extra descriptions are formed as our proposed ViPC-Text dataset. Several examples of the corresponding point clouds, images and texts are displayed in Fig. 4. The extracted latent features can be applied at multiple stages of the completion

model to enhance the multimodal fusion. The subsequent quantitative experiments and visual comparison show the effectiveness of the extracted latent features.

3.4 LLM-assisted 3D Component Corpus

Obviously, text description, as a kind of modality information, can accurately describe the geometric appearance of 3D point clouds, and it is relatively easy to obtain a simple text description for a given 3D shape. It has been demonstrated in [54], [55], [58], [59] that it is feasible to use a text description to improve the understanding of point clouds. In these works, the text descriptions constructed to describe the 3D shape are simple and coarser-grained. Notably, incomplete shapes are more likely to be missing several components and the more accurate and fine-grained geometric descriptions are necessary for the task of point cloud completion. It is extremely difficult to construct a rich, accurate and detailed text corpus for a large number of 3D shapes, which requires a lot of manual annotations. Therefore, in this paper, we construct a fine-grained geometric text corpus for describing components of 3D shapes from the existing ShapeNet-ViPC dataset by using BLIP-2 [60], which belongs to large-scale language models (LLMs). It should be emphasized that the entire construction process is automatic and efficient.

As shown in Fig. 3, taking the chair model as an example, we show the pipeline of fine-grained geometric corpus generation. Generally, BLIP-2 [60] receives an image and question of textual prompt and outputs an answer of textual prompt. In order to adapt BLIP-2 [60] to describe the fine-grained geometric appearance of 3D shapes, we use the following series of language prompts:

Category Question Answering. For a coarse-grained description of shape appearance, we construct a category-related question.

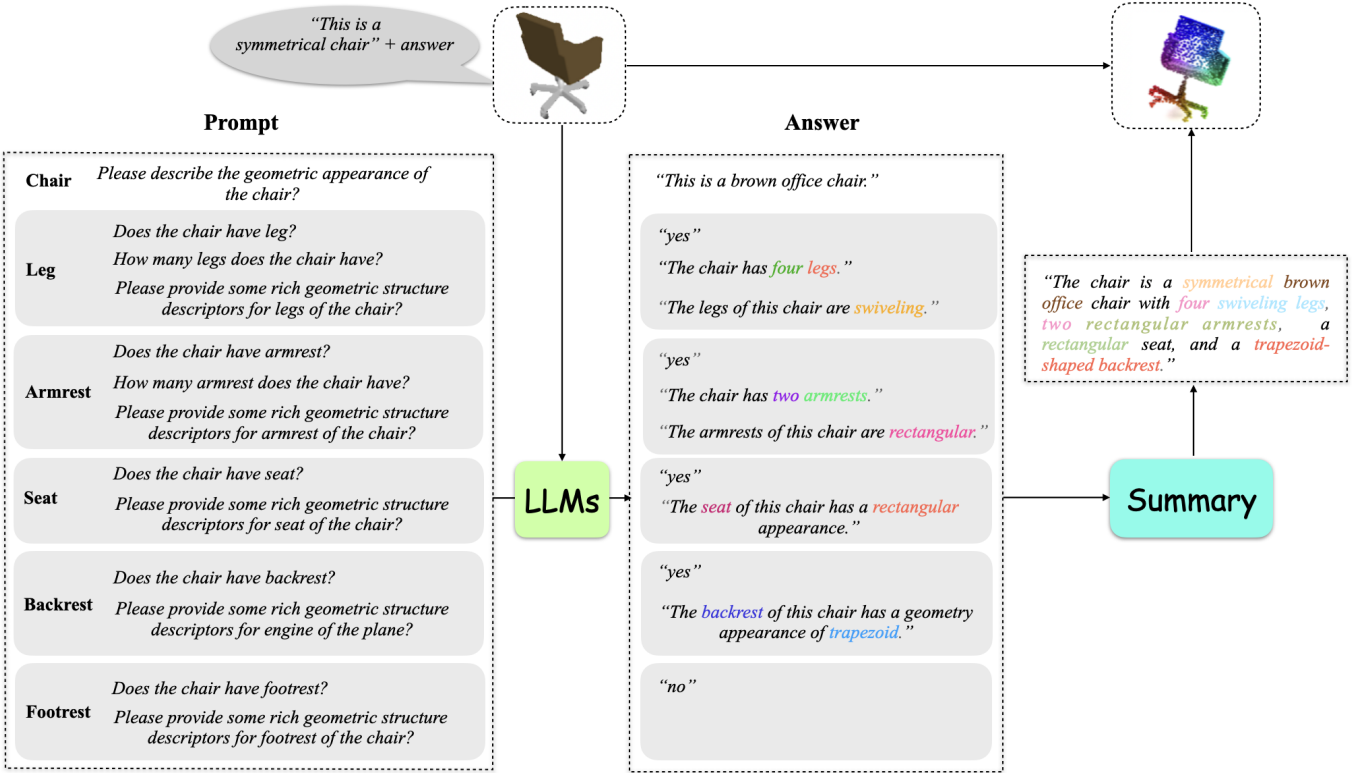


Fig. 3. LLM-assisted 3D component corpus. We feed a query image and a series of part-related language commands into the pre-trained LLMs, which can automatically determine whether each component exists, and generate textual geometric descriptions for each component of the image.

e.g., Input: "Please describe the geometric appearance of the [chair]?"; Output: "This is a brown office [chair].".

Existence Question Answering. In order to judge whether a certain component exists in a given 3D shape, we designed an existence question, which can help us combine the output descriptions of multiple components efficiently. e.g., Input: "Does the [chair] have [leg]?"; Output: "yes or no.".

Quantity Question Answering. In order to more accurately describe the quantity of a certain component for a given 3D shape, we design a question for the number of a certain component. e.g., Input: "How many [leg] does the [chair] have?"; Output: "The [chair] has four [legs].".

Appearance Question Answering. For a fine-grained description of component appearance, we construct a component-related question. e.g., Input: "Please provide some rich geometric structure descriptors for [seat] of the [chair]?"; Output: "The [seat] of this [chair] has a rectangular appearance".

Finally, we summarize the multiple outputs to form a fine-grained geometric appearance description of 3D shapes. In fact, due to the length of text descriptions generated by BLIP-2 [60] always exceeds 258 words, we use the natural language denoising network Bart [61] to compress the length of text description to 50-58. In addition, in order to speed up the generation process of 3D prompts, we just select a random image under 24 views corresponding to each point cloud model as the input image of BLIP-2 [60]. The output text description generated by BLIP-2 [60] is then

considered as the average text description overall 24 viewpoints for a given point cloud. Besides, we design different components for 13 categories utilized throughout the experiment (Fig. 5 gives more details about the categories of the components).

3.5 A Multi-stage Fusion Strategy

Given the global features G_i and G_t that are respectively extracted from the visual and textual encoders of the multimodal feature extraction module, our aim is to fuse these multimodal features into our basic network to enhance the ability of the basic network to understand the structure and semantics of the incomplete 3D shapes. As shown in Fig. 2, we perform the strategy of two-stage multimodal feature fusion in the basic network, where the first fusion operation is performed before fine-grained cross-attention fusion and the second one is performed after the attention fusion.

Specifically, at the first stage of multimodal feature fusion, we concatenate the textual features G_i and visual features G_t together. Then, we repeat these multimodal features and concatenate the features with fine-grained point cloud features $F_p \in R^{256 \times 128}$. Subsequently, the operation of shared *MLPs* is performed to achieve the fusion of multimodal features and the output can be denoted as $y_1 \in R^{256 \times 128}$. After the first multimodal fusion, we fuse the fine-grained image features F_i with the multimodal features y_1 . Here, the operation of cross-attention is used to achieve the fine-grained feature fusion, and the output is denoted as $y_2 \in R^{256 \times 128}$. Then, we use the fine-grained feature y_2 to perform the second fusion with multimodal features G_i and G_t . Since the process of the second fusion is similar to the first one, the introduction is omitted here. The output by the second stage is denoted as $y_3 \in R^{256 \times 128}$.

TABLE 1

Quantitative comparisons to state-of-the-art methods on known eight categories of ShapeNet-ViPC dataset by using Mean Chamfer Distance per point ($\times 10^{-3}$) with 2048 points. The best is highlighted in bold. * means the code is not available or uncompleted.

Methods	Mean CD per point (lower is better)								
	Mean	Airplane	Cabinet	Car	Chair	Lamp	Sofa	table	Watercraft
Unimodal Methods									
AtlasNet [62]	6.062	5.032	6.414	4.868	8.161	7.182	6.023	6.561	4.261
FoldingNet [63]	6.271	5.242	6.958	5.307	8.823	6.504	6.368	7.080	3.882
PCN [43]	5.619	4.246	6.409	4.840	7.441	6.331	5.668	6.508	3.510
TopNet [44]	4.976	3.710	5.629	4.530	6.391	5.547	5.281	5.381	3.35
ECG [64]	4.957	2.952	6.721	5.243	5.867	4.602	.813	4.332	3.127
VRC-Net [65]	4.598	2.813	6.108	4.932	5.342	4.103	6.614	3.953	2.925
PF-Net [66]	3.873	2.515	4.453	3.602	4.478	5.185	4.113	3.838	2.871
MSN [45]	3.793	2.038	5.06	4.322	4.135	4.247	4.183	3.976	2.379
GRNet [67]	3.171	1.916	4.468	3.915	3.402	3.034	3.872	3.071	2.160
PoinTr [49]	2.851	1.686	4.001	3.203	3.111	2.928	3.507	2.845	1.737
PointAttN [68]	2.853	1.613	3.969	3.257	3.157	3.058	3.406	2.787	1.872
SDT [69]	4.246	3.166	4.807	3.607	5.056	6.101	4.525	3.995	2.856
Seedformer [51]	2.902	1.716	4.049	3.392	3.151	3.226	3.603	2.803	1.679
Multimodal Methods									
ViPC [16]*	3.308	1.760	4.558	3.183	2.476	2.867	4.481	4.990	2.197
CSDN [18]*	2.570	1.251	3.670	2.977	2.835	2.554	3.240	2.575	1.742
XMFNet [17]	1.443	0.572	1.980	1.754	1.403	1.810	1.702	1.386	0.945
Ours	1.159	0.539	1.793	1.599	1.193	0.729	1.512	1.151	0.756

TABLE 2

Quantitative comparisons to state-of-the-art methods on known eight categories of ShapeNet-ViPC dataset by using Mean F-Score @ 0.001 with 2048 points. The best is highlighted in bold. * means the code is not available or uncompleted.

Methods	F-Score@0.001 (higher is better)								
	Mean	Airplane	Cabinet	Car	Chair	Lamp	Sofa	table	Watercraft
Unimodal Methods									
AtlasNet [62]	0.410	0.509	0.304	0.379	0.326	0.426	0.318	0.469	0.551
FoldingNet [63]	0.331	0.432	0.237	0.300	0.204	0.360	0.249	0.351	0.518
PCN [43]	0.407	0.578	0.27	0.331	0.323	0.456	0.293	0.431	0.577
TopNet [44]	0.467	0.593	0.358	0.405	0.388	0.491	0.361	0.528	0.615
ECG [64]	0.704	0.880	0.542	0.713	0.671	0.689	0.534	0.792	0.810
VRC-Net [65]	0.764	0.902	0.621	0.753	0.722	0.823	0.654	0.810	0.832
PF-Net [66]	0.551	0.718	0.399	0.453	0.489	0.559	0.409	0.614	0.656
MSN [45]	0.578	0.798	0.378	0.380	0.562	0.652	0.410	0.615	0.708
GRNet [67]	0.601	0.767	0.426	0.446	0.575	0.694	0.450	0.639	0.704
PoinTr [49]	0.683	0.842	0.516	0.545	0.662	0.742	0.547	0.723	0.780
PointAttN [68]	0.662	0.841	0.483	0.515	0.638	0.729	0.512	0.699	0.774
SDT [69]	0.473	0.636	0.291	0.363	0.398	0.442	0.307	0.574	0.602
Seedformer [51]	0.688	0.835	0.551	0.544	0.668	0.777	0.555	0.716	0.786
Multimodal Methods									
ViPC [16]*	0.591	0.803	0.451	0.512	0.529	0.706	0.434	0.594	0.730
CSDN [18]*	0.695	0.862	0.548	0.560	0.669	0.761	0.557	0.729	0.782
XMFNet [17]	0.796	0.961	0.662	0.691	0.809	0.792	0.723	0.830	0.901
Ours	0.842	0.971	0.705	0.729	0.844	0.924	0.767	0.862	0.935

our corpus are range in 50-58, which is relatively concise. The concise text can be directly used as the input of the CLIP model, which can only accept the input of the token length less than 77. It should be emphasized that our text description is relatively concise, but our corpus contains a variety of vocabulary related to geometric descriptions to accurately describe 3D shapes. The word cloud of the chair category in the corpus is shown in Fig. 6, our corpus contains a broad vocabulary related to number of shape components and the geometric appearance of 3D shapes.

4.2 Implementation Details

Corpus Generation. The corpus generation algorithm is implemented on a single NVIDIA RTX A6000. In fact, the algorithm takes about 26G GPU memory and cost an average of 1 to 4 seconds to generate one item of text description from an image.

Network Training. During training, we use the same training setting as XMFNet [17]. Our method is implemented using PyTorch framework [70] and all our experiments are performed on a 4 GPU NVIDIA A800-SXM4-80G cluster with 320G GPU memory,

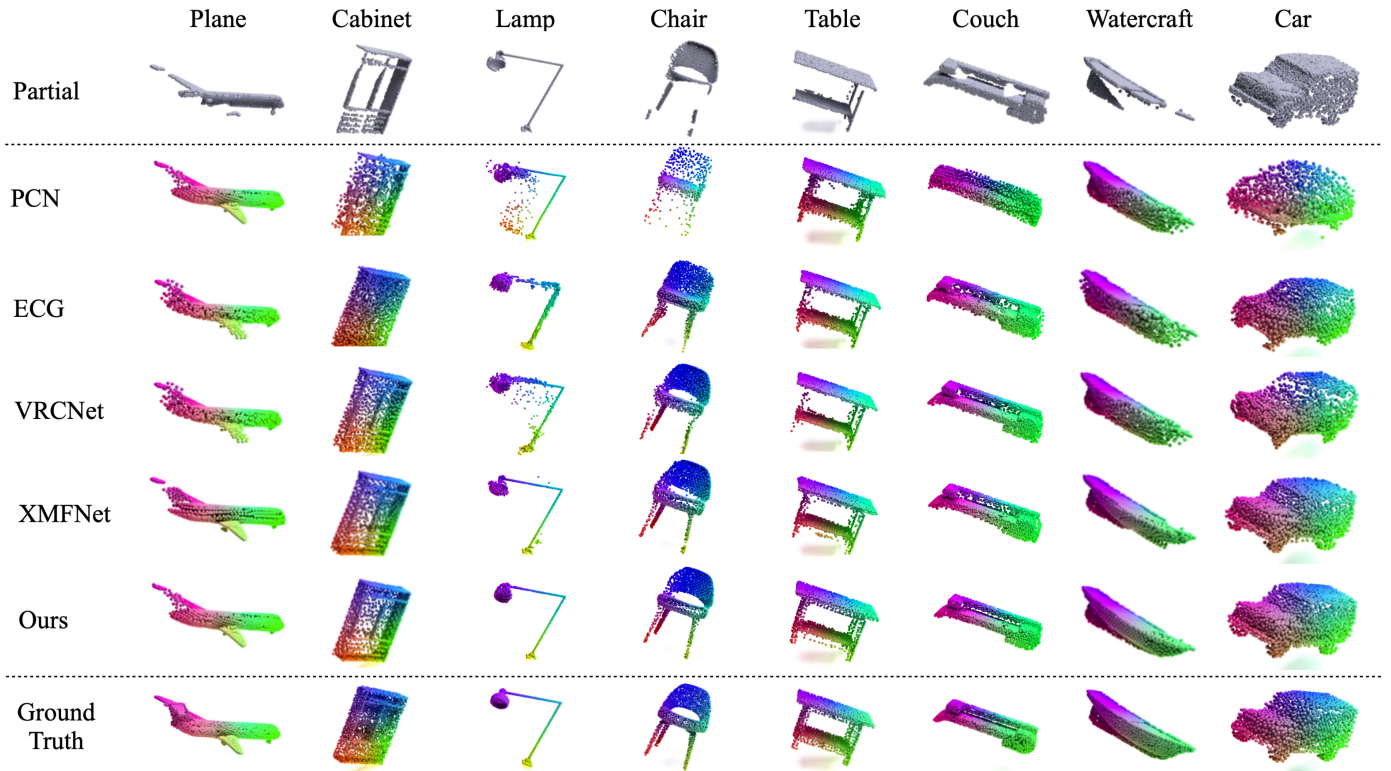


Fig. 7. Qualitative comparisons between different methods including both the unimodal methods (PCN [43], ECG [64], VRCNet [65]) and multimodal methods (XMFNet [17] and our method).

occupying about 160G cluster’s GPU memory when running in parallel. We use Adam optimizer [71] with $\beta_1 = 0.9$ and $\beta_2 = 0.999$. The model is trained for 400 epochs with a batch size of 560 and an initial learning rate of 0.00209.

4.3 Comparisons on ShapeNet-ViPC Dataset

4.3.1 Comparisons on Known Categories

In this section, we compare our method with other unimodal and multimodal methods. First, to quantitatively evaluate the performance of multiple methods, we use CD and F-score as metrics for the reconstruction quality on the ShapeNet-ViPC dataset. The evaluation metrics are similar to XMFNet [17]. Tab. 1 and Tab. 2 report the quantitative results of multiple methods and it can be clearly seen that our method has great advantages over both unimodal and multimodal methods. Especially compared with the state-of-the-art multimodal fusion method XMFNet, our results show a significant improvement. Then, the qualitative comparisons are shown in Fig. 7. Similar to XMFNet [17], we compare our method with several unimodal completion methods including PCN [43], ECG [64], VRCNet [65], while for the multimodal method, we only compare with XMFNet [17] for the reason that the code of ViPC is incomplete and the code of CSDN is not available. First of all, compared with other methods, our method can produce complete shapes with less noise points. Then, according to the visualization results, the proposed network has a stronger ability to predict the semantic information of missing parts and the reconstruction quality of the missing parts are more accurate. As shown in Fig. 7, our method can reconstruct a more complete aircraft tail and lampshade for the airplane and lamp models respectively. And for car model in Fig. 7, our method can also reconstruct more accurate car tires. In addition, thanks

TABLE 3
Quantitative comparisons to state-of-the-art methods on unknown five categories of ShapeNet-ViPC dataset by using Mean Chamfer Distance per point ($\times 10^{-3}$) with 2048 points. The best is highlighted in bold.

Methods	Mean CD per point (lower is better)				
	Mean	Bench	Monitor	Speaker	Phone
PF-Net [66]	5.011	3.684	5.304	7.663	3.392
MSN [45]	4.684	2.613	4.818	8.259	3.047
GRNet [67]	4.096	2.367	4.102	6.493	3.422
PoinTr [49]	3.755	1.976	4.084	5.913	3.049
ViPC [16]	4.601	3.091	4.419	7.674	3.219
PointAttN [68]	3.674	2.135	3.741	5.973	2.848
SDT [69]	6.001	4.096	6.222	9.499	4.189
CSDN [18]	3.656	1.834	4.115	5.690	2.985
XMFNet [17]	3.259	1.512	3.668	5.417	2.439
Ours	3.098	1.217	3.043	5.311	2.819

to the introduction of rich text information in our work, we can also predict the geometric structure of shapes more accurately than other methods. The Fig. 7 clearly shows that the slender structure of a lamp, the complex structure of the chair back, the flat structure of the table pedal and the corner of the watercraft head can all be better reconstructed compared with other methods. Therefore, in summary, our method is capable of producing cleaner, more structured and more semantic completions than the other methods.

4.3.2 Comparisons on Novel Categories

To demonstrate the generalization ability of the proposed method, we also show the quantitative and qualitative results of five unknown categories on the ShapeNet-ViPC dataset [16]. Specif-

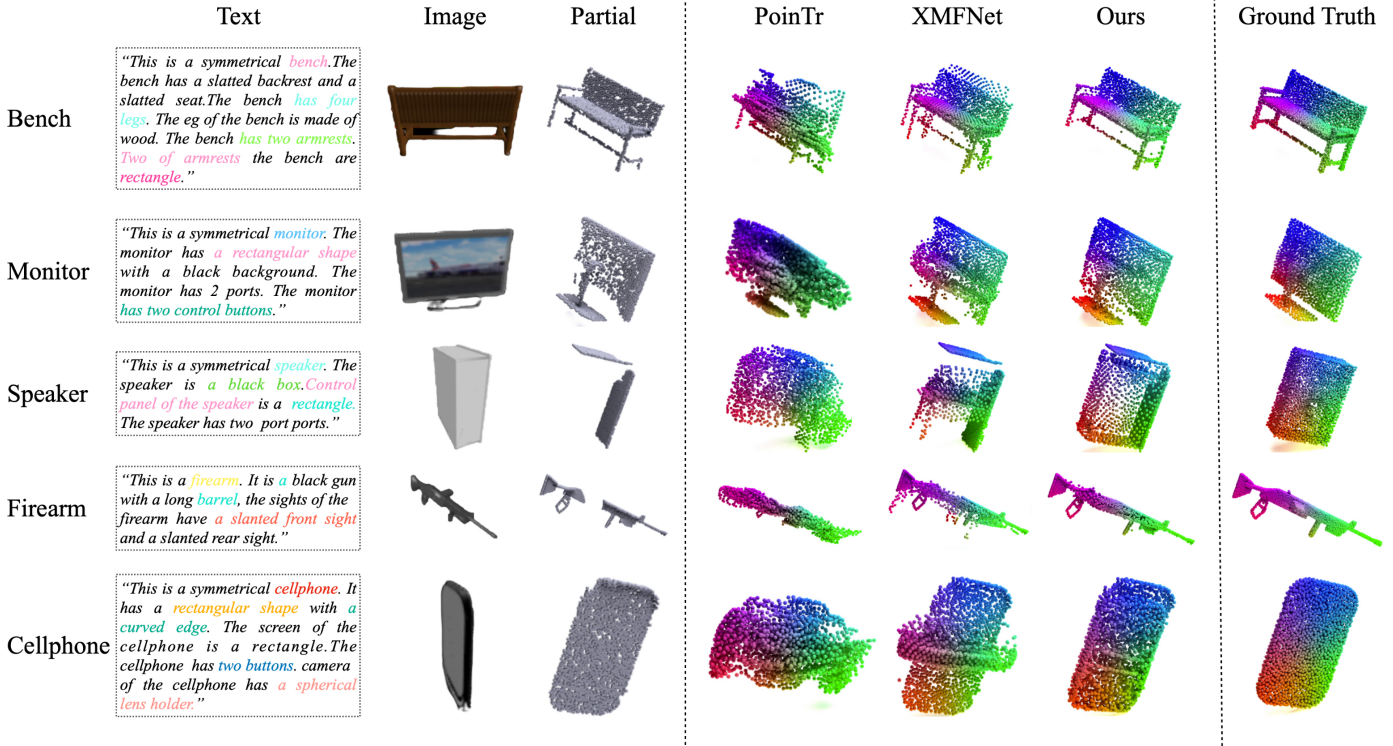


Fig. 8. Visual comparisons of recent point cloud completion methods [17], [49] and ours on unseen categories of ShapeNet-ViPC [16]. Our method produces the most complete and detailed structures compared to its competitors.

TABLE 4

Quantitative comparisons to state-of-the-art methods on unknown five categories of ShapeNet-ViPC dataset by using Mean F-Score @ 0.001 with 2048 points. The best is highlighted in bold.

Methods	F-Score@0.001 (higher is better)				
	Mean	Bench	Monitor	Speaker	Phone
PF-Net [66]	0.468	0.584	0.433	0.319	0.534
MSN [45]	0.533	0.706	0.527	0.291	0.607
GRNet [45]	0.548	0.711	0.537	0.376	0.569
PoinTr [49]	0.619	0.797	0.599	0.454	0.627
ViPC [16]	0.498	0.654	0.491	0.313	0.535
PointAttN [68]	0.605	0.764	0.591	0.428	0.637
SDT [69]	0.327	0.479	0.268	0.197	0.362
CSDN [18]	0.631	0.798	0.598	0.485	0.644
XMFNet [17]	0.664	0.830	0.622	0.517	0.687
Ours	0.687	0.872	0.656	0.542	0.678

ically, for all methods that need to be compared, we train the more general models by using the known 8 categories on the ShapeNet-ViPC dataset [16], then we evaluate these models on the 4 unknown categories (Actually the same as CSDN [18], we only tested four unknown categories of objects). Still using the same metrics, the quantitative results of CD and F-Score are reported in Tab. 3 and Tab. 4, respectively. Our approach still outperforms state-of-the-art unimodal methods such as PointAttN [68] and PoinTr [49] as well as multimodal method XMFNet [17]. Besides, we also present a visual comparison between our method and other methods including a Transformer-based method PoinTr [49] and a multimodal-based method XMFNet [17], as shown in Fig. 8. We can observe that PoinTr [49] cannot well recover the missing

shapes for previously unseen categories, although it achieves competitive performance on quantitative results. Then, only with the help of image auxiliary information, the completed shapes produced by XMFNet [17] suffer from poor quality. In contrast, our method can produce clear results with stronger structural details. This comparison further demonstrates that our method successfully exploits the complementary information provided by the images and text for point cloud completion.

4.4 Ablation Study

4.4.1 Performance of Multimodal Information

The performance of G_i . As shown in the first and second rows of Tab. 5 and Tab. 6, we conduct an ablation study to access the effectiveness of the visual encoder of CLIP. Here, we only fuse the visual global features G_i with the fine-grained features of incomplete point clouds. It should be noted that the input image used in CLIP is the same as the input in the baseline model. Compared with the baseline (XMFNet [17]), the introduction of the visual global feature in the CLIP can achieve 16.42% and 4.90% performance for the metrics of CD and F-Score on the known categories of ShapeNet-ViPC dataset [16]. This experiment can verify that the visual module of the CLIP can deliver more generalized visual information compared with the fine-grained image features in the baseline, thereby achieving a significant improvement.

The performance of G_t . Compared to visual information, the semantic description text for point clouds is more readily available in practical applications. To verify the validity of the introduction of text information, we use a simple text to guide the process of

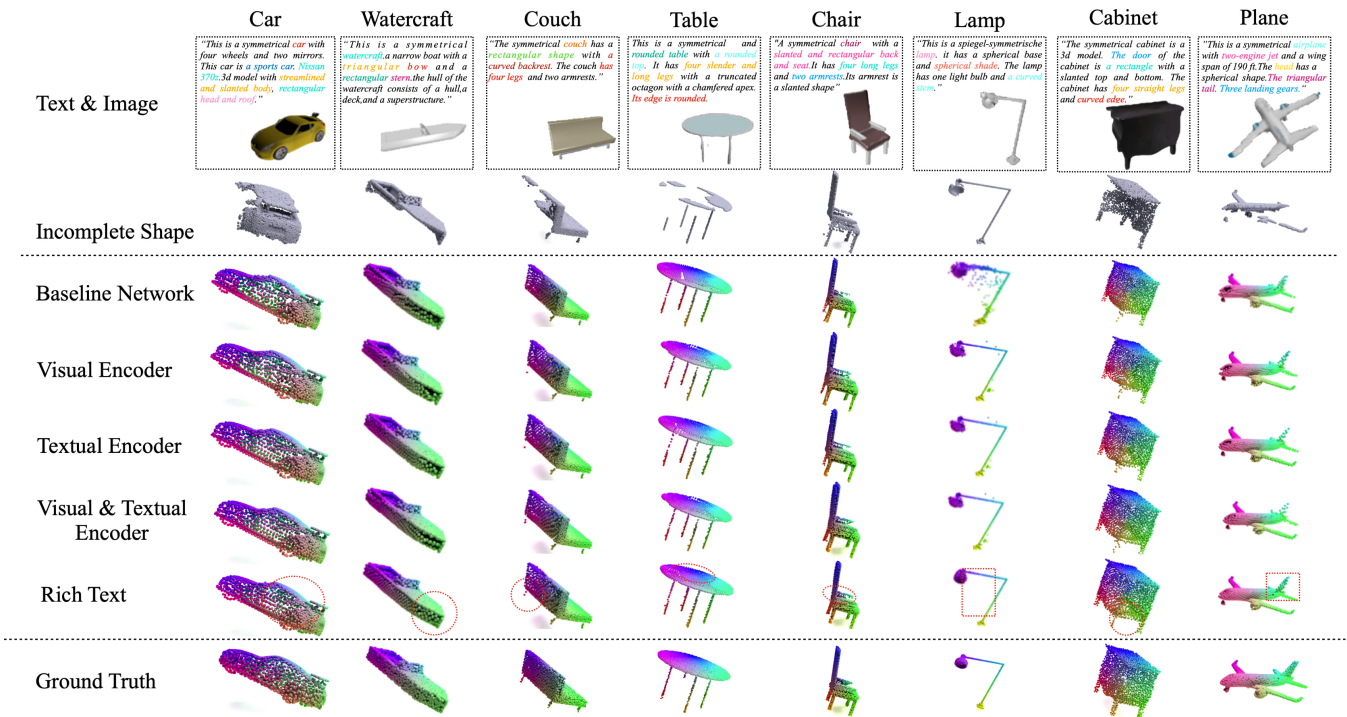


Fig. 9. Visualized ablation study of eight known category objects on ShapeNet-ViPC dataset. The first row shows descriptions of the complex text; Rows 2-3 show the incomplete point clouds and the rendered image; Rows 4-9 show the visualization results under the use of different modal information; The last row gives the ground truth.

TABLE 5

Ablation studies for the multimodal information used in our network on the ShapeNet-ViPC dataset. The Chamfer Distance is used as the metric for evaluating the gains from different multimodal information and different fusion strategies.

Ablation	Fusion Stage 1	Fusion Stage 2	Mean CD per point $\times 10^{-3}$ (lower is better)									
			Mean	Improv.(%)	Airplane	Cabinet	Car	Chair	Lamp	Sofa	table	Watercraft
Baseline (XMFNet [17])	-	-	1.443	-	0.572	1.980	1.754	1.403	1.810	1.702	1.386	0.945
w/ Visual Encoder	✓	✓	1.206	16.42	0.546	1.859	1.717	1.227	0.790	1.539	1.181	0.786
w/ Text Encoder	✓	✓	1.251	13.31	0.564	1.814	1.736	1.346	0.881	1.554	1.320	0.791
w/ Visual Encoder & Text Encoder	✓	✓	1.190	17.53	0.546	1.808	1.682	1.204	0.791	1.545	1.153	0.787
	✓	✓	1.188	17.67	0.542	1.830	1.690	1.181	0.791	1.541	1.144	0.786
Final(w/ Rich Text)	✓	✓	1.181	18.16	0.552	1.808	1.634	1.214	0.740	1.538	1.176	0.788
Final(w/ Rich Text)	✓	✓	1.159	19.68	0.539	1.793	1.599	1.193	0.729	1.512	1.151	0.756

TABLE 6

Ablation studies for the multimodal information used in our network on the ShapeNet-ViPC dataset. The Mean F-Score @ 0.001 is used as the metric for evaluating the gains from different multimodal information and different fusion strategies.

Ablation	Fusion Stage 1	Fusion Stage 2	F-Score@0.001 (higher is better)									
			Mean	Improv.(%)	Airplane	Cabinet	Car	Chair	Lamp	Sofa	table	Watercraft
Baseline (XMFNet [17])	-	-	0.796	-	0.961	0.662	0.691	0.809	0.792	0.723	0.830	0.901
w/ Visual Encoder	✓	✓	0.835	4.90	0.969	0.695	0.709	0.839	0.914	0.762	0.859	0.929
w/ Text Encoder	✓	✓	0.823	3.39	0.967	0.700	0.699	0.814	0.890	0.757	0.831	0.929
w/ Visual Encoder & Text Encoder	✓	✓	0.831	4.40	0.929	0.698	0.712	0.842	0.914	0.758	0.863	0.929
	✓	✓	0.836	5.03	0.970	0.694	0.710	0.844	0.915	0.760	0.864	0.930
Final(w/ Rich Text)	✓	✓	0.838	5.28	0.968	0.703	0.722	0.840	0.922	0.763	0.860	0.930
Final(w/ Rich Text)	✓	✓	0.842	5.78	0.971	0.705	0.729	0.844	0.924	0.767	0.862	0.935

the point cloud completion task. In fact, we only use the simple prompt “This is a [category]” as the input of our multimodal feature extraction module. The experimental results in the first and third rows of Tab. 5 and Tab. 6 show that this simple global textual template is also useful for guiding the process of point cloud completion. As reported, the improvements of 13.31% and 3.39% can be accessed for the metrics of CD and F-Score, respectively.

Therefore, the performances illustrate that just a simple text related to the object category can provide effective semantic information.

The performance of $G_i + G_t$. Considering the complementarity between the multimodal information, we also conduct an ablation study to verify the effectiveness of the textual and visual information fusion. As reported in the first and sixth rows of Tab. 5

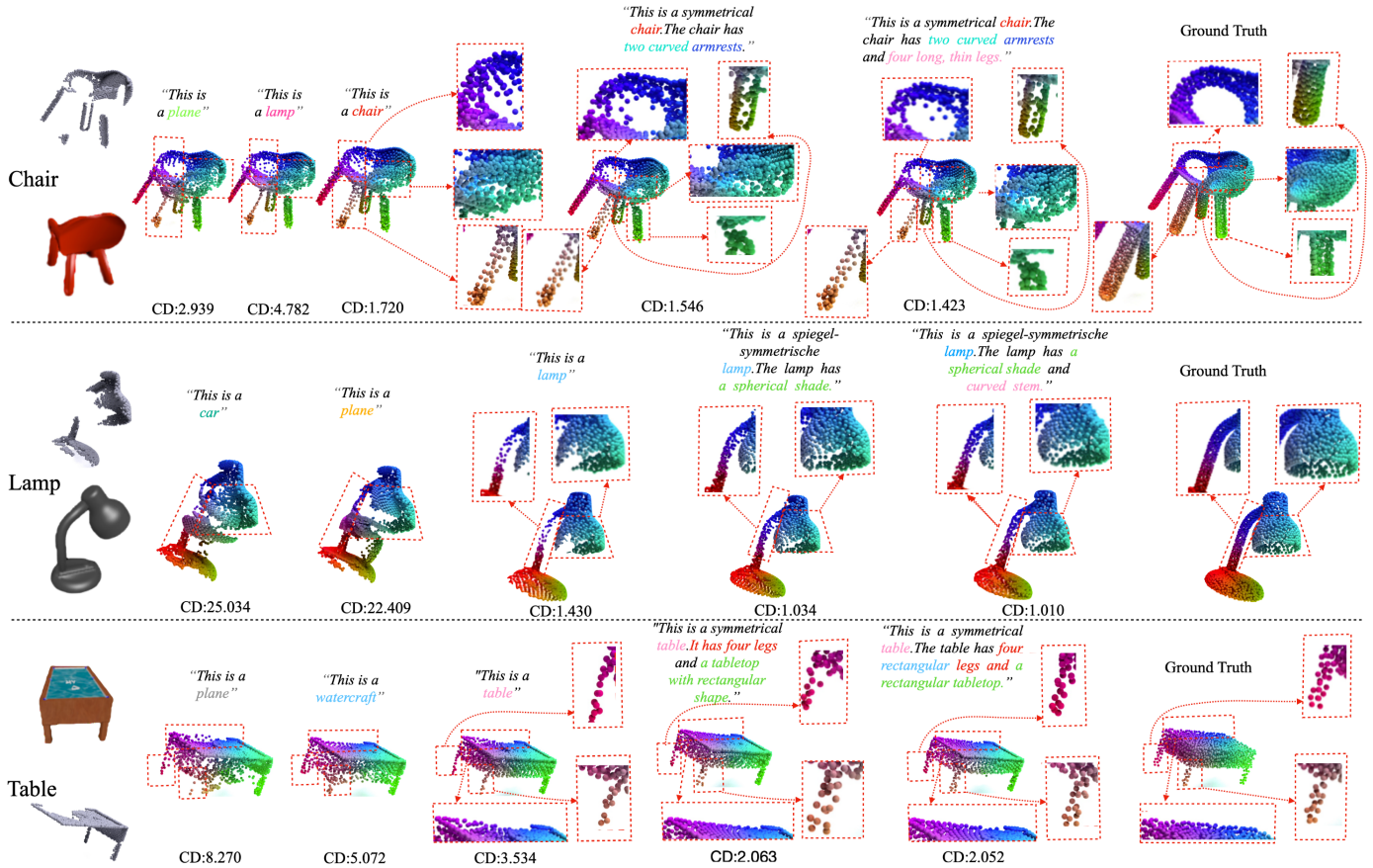


Fig. 10. Ablation study of various textual information. From left to right, we gradually increase the text description information (wrong text information is given on the left, and accurate description details are given on the right), and the quality of the complete shapes is improved. In addition, the values below each example are the CD metric for evaluating the reconstruction quality between different text descriptions.

and Tab. 6, when visual information and simple text information are both fused into our completion network, the improvements of 18.16% and 5.28% can be accessed for the metrics of CD and F-Score, respectively. This demonstrates that the complementarity among the three modal information of point cloud, image, and text description exists, and the quality of the reconstruction 3D shape can be better improved by using the three modal information at the same time. In addition, we also verified the effectiveness of fine-grained geometric description text information, as shown in the last two rows of the Tab. 5 and Tab. 6, compared to the simple text, text description used in our ViPC-Text dataset can bring 1.86% and 0.48% improvements for the metrics of CD and F-Score. Ultimately, our method can access 19.68% and 5.78% improvement compared to the XMFNet [17]. Furthermore, as shown in the red dashed box of Fig. 9, our method with rich text descriptions has more advantages in structure and detail reconstruction. Our reconstruction results are sharper and the distribution of points is more uniform.

4.4.2 The Strategy of Multi-Stage Fusion

As shown in the fourth to sixth rows of Tab. 5 and Tab. 6, we show an ablation study to explore the strategies for multimodal feature fusion. Specifically, we compare three fusion strategies as follows:

- Multimodal feature fusion is done before fine-grained fusion on top of the baseline.
- Multimodal feature fusion is done after fine-grained fusion on top of the baseline.

- Multimodal feature fusion is performed in two stages, before and after fine-grained fusion on top of the baseline.

Through meticulous experimental comparisons, we found that the most effective fusion strategy for point cloud completion is to choose the third one described above, which adopts two-stage fusion and can better extract complementary information among multimodal information.

4.4.3 The performance of various text descriptions

In this section, we design various text descriptions to explore the impact of text richness on the final complete results. As shown in Fig. 10, we select three shapes from different categories to explore the effectiveness of the added textual information. First of all, we use simple text descriptions (e.g. "This is a [chair]") to explore the influence of the textual information on the final complete shapes. Specifically, we compare visualization of the complete shapes predicted from correct and incorrect textual information. We found that misleading semantic text descriptions can severely affect model performance. The CD values below the instances are consistent with the visual results. In addition, we compared the impact of simple text descriptions and rich text descriptions on final complete shapes. The visualization shows that rich text information can provide the completion network with more additional geometric and semantic information than simple text descriptions. For example, for the lamp model in Fig. 10, the input of rich text description can improve the reconstruction quality of the cap and stem compared with the simple text description. For the chair

model in Fig. 10, our network can predict the cleaner arms and legs when rich texts are used as the input. For the table model in Fig. 10, the rich text can improve reconstruction quality of tabletop and make the structure of the table legs closer to the rectangular structure. Consistently, the CD values under these visual examples can also reflect the effectiveness of rich text descriptions. Finally, we also tried to construct more precise hand-crafted descriptions to each example, as shown in the penultimate column of Fig. 10. It can be seen that a finer description can indeed improve the reconstruction accuracy of the incomplete shape. This also indicates that the text modality plays an important role in the task of point cloud completion.

5 CONCLUSION

In this paper, based on the CLIP model, we propose a novel multimodal fusion architecture called FTPNet for 3D point cloud completion. Different from existing multimodal methods, we introduce textual description into the completion architecture. Then, to further explore the function of textual information on the quality of 3d shape completion, we design an automatic fine-grained text generation method that can construct a multi-category fine-grained text corpus. Extensive experiments demonstrate that fine-grained text descriptions can dramatically improve our FTPNet's ability to understand the semantics and structure information of 3D shapes. However, our method still has some drawbacks where the model's ability to understand the fine-grained text information is still poor. In the future, we will further explore the relationship between point cloud completion and fine-grained text, and build a fine-grained and controllable text-guided 3D point cloud completion framework.

ACKNOWLEDGMENTS

The authors would like to thank the High Performance Computing Center of Dalian Maritime University for providing the computing resources. Jun Zhou is supported by NSFC Fund (No. 62002040) and China Postdoctoral Science Foundation (No. 2021M690501). Xiuping Liu is supported by NSFC Fund (No. 61976040). Mingjie Wang is supported by the Science Foundation of Zhejiang Sci-Tech University (No. 22062338-Y). Hongchen Tan is supported by National Natural Science Foundation of China (No. 62201020) and Beijing Postdoctoral Science Foundation (No. 2022-ZZ-069).

REFERENCES

- [1] F. Pomerleau, F. Colas, and R. Siegwart, "A review of point cloud registration algorithms for mobile robotics," *Foundations and Trends in Robotics*, vol. 4, no. 1, pp. 1–104, 2015.
- [2] S. Kato, S. Tokunaga, Y. Maruyama, S. Maeda, M. Hirabayashi, Y. Kitsukawa, A. Monroy, T. Ando, Y. Fujii, and T. Azumi, "Autoware on board: enabling autonomous vehicles with embedded systems," in *2018 ACM/IEEE 9th International Conference on Cyber-Physical Systems (ICCPs)*, Aug 2018. [Online]. Available: <http://dx.doi.org/10.1109/iccps.2018.00035>
- [3] Q. Wang and M.-K. Kim, "Applications of 3d point cloud data in the construction industry: A fifteen-year review from 2004 to 2018," *Advanced Engineering Informatics*, vol. 39, pp. 306–319, 2019.
- [4] J. Hou, A. Dai, and M. Nießner, "3d-sis: 3d semantic instance segmentation of rgb-d scans," in *Proceedings of the IEEE/CVF conference on computer vision and pattern recognition*, 2019, pp. 4421–4430.
- [5] L. J. Wells, R. Dastoorian, and J. A. Camelio, "A novel nurbs surface approach to statistically monitor manufacturing processes with point cloud data," *Journal of Intelligent Manufacturing*, vol. 32, pp. 329–345, 2021.
- [6] Z. Ma and S. Liu, "A review of 3d reconstruction techniques in civil engineering and their applications," *Advanced Engineering Informatics*, vol. 37, pp. 163–174, 2018.
- [7] P. Mandikal and V. B. Radhakrishnan, "Dense 3d point cloud reconstruction using a deep pyramid network," in *2019 IEEE Winter Conference on Applications of Computer Vision (WACV)*. IEEE, 2019, pp. 1052–1060.
- [8] J. Choe, B. Joung, F. Rameau, J. Park, and I. S. Kweon, "Deep point cloud reconstruction," *arXiv preprint arXiv:2111.11704*, 2021.
- [9] E. Grilli, F. Menna, and F. Remondino, "A review of point clouds segmentation and classification algorithms," *The International Archives of Photogrammetry, Remote Sensing and Spatial Information Sciences*, vol. 42, p. 339, 2017.
- [10] Y. Guo, H. Wang, Q. Hu, H. Liu, L. Liu, and M. Bennamoun, "Deep learning for 3d point clouds: A survey," *IEEE transactions on pattern analysis and machine intelligence*, vol. 43, no. 12, pp. 4338–4364, 2020.
- [11] D. Fernandes, A. Silva, R. Névoa, C. Simões, D. Gonzalez, M. Guevara, P. Novais, J. Monteiro, and P. Melo-Pinto, "Point-cloud based 3d object detection and classification methods for self-driving applications: A survey and taxonomy," *Information Fusion*, vol. 68, pp. 161–191, 2021.
- [12] L. Li, R. Wang, and X. Zhang, "A tutorial review on point cloud registrations: principle, classification, comparison, and technology challenges," *Mathematical Problems in Engineering*, vol. 2021, pp. 1–32, 2021.
- [13] S. S. Mohammadi, Y. Wang, and A. Del Bue, "Pointview-gcn: 3d shape classification with multi-view point clouds," in *2021 IEEE International Conference on Image Processing (ICIP)*. IEEE, 2021, pp. 3103–3107.
- [14] H. Wang, L. Ding, S. Dong, S. Shi, A. Li, J. Li, Z. Li, and L. Wang, "CAGroup3d: Class-aware grouping for 3d object detection on point clouds," in *Advances in Neural Information Processing Systems*, A. H. Oh, A. Agarwal, D. Belgrave, and K. Cho, Eds., 2022. [Online]. Available: <https://openreview.net/forum?id=nLKKHwYP4Au>
- [15] T. Zhou, S. M. Hasheminasab, and A. Habib, "Tightly-coupled camera/lidar integration for point cloud generation from gnss/ins-assisted uav mapping systems," *ISPRS Journal of Photogrammetry and Remote Sensing*, vol. 180, pp. 336–356, 2021.
- [16] X. Zhang, Y. Feng, S. Li, C. Zou, H. Wan, X. Zhao, Y. Guo, and Y. Gao, "View-guided point cloud completion," in *Proceedings of the IEEE/CVF Conference on Computer Vision and Pattern Recognition*, 2021, pp. 15 890–15 899.
- [17] E. Aiello, D. Valsesia, and E. Magli, "Cross-modal learning for image-guided point cloud shape completion," *arXiv preprint arXiv:2209.09552*, 2022.
- [18] Z. Zhu, L. Nan, H. Xie, H. Chen, J. Wang, M. Wei, and J. Qin, "Csdn: Cross-modal shape-transfer dual-refinement network for point cloud completion," *IEEE Transactions on Visualization and Computer Graphics*, 2023.
- [19] J. Devlin, M.-W. Chang, K. Lee, and K. Toutanova, "Bert: Pre-training of deep bidirectional transformers for language understanding," in *Proceedings of the 2019 Conference of the North, Jan 2019*. [Online]. Available: <http://dx.doi.org/10.18653/v1/n19-1423>
- [20] T. Brown, B. Mann, N. Ryder, M. Subbiah, J. D. Kaplan, P. Dhariwal, A. Neelakantan, P. Shyam, G. Sastry, A. Askell *et al.*, "Language models are few-shot learners," *Advances in neural information processing systems*, vol. 33, pp. 1877–1901, 2020.
- [21] T. Xu, P. Zhang, Q. Huang, H. Zhang, Z. Gan, X. Huang, and X. He, "Attgan: Fine-grained text to image generation with attentional generative adversarial networks," in *Proceedings of the IEEE conference on computer vision and pattern recognition*, 2018, pp. 1316–1324.
- [22] H. Zhang, J. Y. Koh, J. Baldrige, H. Lee, and Y. Yang, "Cross-modal contrastive learning for text-to-image generation," in *Proceedings of the IEEE/CVF conference on computer vision and pattern recognition*, 2021, pp. 833–842.
- [23] A. Nichol, P. Dhariwal, A. Ramesh, P. Shyam, P. Mishkin, B. McGrew, I. Sutskever, and M. Chen, "Glide: Towards photorealistic image generation and editing with text-guided diffusion models," *arXiv preprint arXiv:2112.10741*, 2021.
- [24] A. Ramesh, M. Pavlov, G. Goh, S. Gray, C. Voss, A. Radford, M. Chen, and I. Sutskever, "Zero-shot text-to-image generation," in *International Conference on Machine Learning*. PMLR, 2021, pp. 8821–8831.
- [25] A. Ramesh, P. Dhariwal, A. Nichol, C. Chu, and M. Chen, "Hierarchical text-conditional image generation with clip latents," *arXiv preprint arXiv:2204.06125*, 2022.
- [26] N. Ruiz, Y. Li, V. Jampani, Y. Pritch, M. Rubinstein, and K. Aberman, "Dreambooth: Fine tuning text-to-image diffusion models for subject-driven generation," in *Proceedings of the IEEE/CVF Conference on Computer Vision and Pattern Recognition*, 2023, pp. 22 500–22 510.
- [27] A. Jain, B. Mildenhall, J. T. Barron, P. Abbeel, and B. Poole, "Zero-shot text-guided object generation with dream fields," in *Proceedings of*

- the *IEEE/CVF Conference on Computer Vision and Pattern Recognition*, 2022, pp. 867–876.
- [28] C. Wang, M. Chai, M. He, D. Chen, and J. Liao, “Clip-nerf: Text-and-image driven manipulation of neural radiance fields,” in *Proceedings of the IEEE/CVF Conference on Computer Vision and Pattern Recognition*, 2022, pp. 3835–3844.
- [29] B. Poole, A. Jain, J. T. Barron, and B. Mildenhall, “Dreamfusion: Text-to-3d using 2d diffusion,” *arXiv preprint arXiv:2209.14988*, 2022.
- [30] C.-H. Lin, J. Gao, L. Tang, T. Takikawa, X. Zeng, X. Huang, K. Kreis, S. Fidler, M.-Y. Liu, and T.-Y. Lin, “Magic3d: High-resolution text-to-3d content creation,” in *Proceedings of the IEEE/CVF Conference on Computer Vision and Pattern Recognition*, 2023, pp. 300–309.
- [31] C. Tsalicoglou, F. Manhardt, A. Tonioni, M. Niemeyer, and F. Tombari, “Textmesh: Generation of realistic 3d meshes from text prompts,” *arXiv preprint arXiv:2304.12439*, 2023.
- [32] Y. Cao, Y.-P. Cao, K. Han, Y. Shan, and K.-Y. K. Wong, “Dreamavatar: Text-and-shape guided 3d human avatar generation via diffusion models,” *arXiv preprint arXiv:2304.00916*, 2023.
- [33] E. Richardson, G. Metzger, Y. Alaluf, R. Giryas, and D. Cohen-Or, “Texture: Text-guided texturing of 3d shapes,” *arXiv preprint arXiv:2302.01721*, 2023.
- [34] J. Zhang, X. Li, Z. Wan, C. Wang, and J. Liao, “Text2nerf: Text-driven 3d scene generation with neural radiance fields,” *arXiv preprint arXiv:2305.11588*, 2023.
- [35] K. Chen, C. B. Choy, M. Savva, A. X. Chang, T. Funkhouser, and S. Savarese, “Text2shape: Generating shapes from natural language by learning joint embeddings,” in *Computer Vision—ACCV 2018: 14th Asian Conference on Computer Vision, Perth, Australia, December 2–6, 2018, Revised Selected Papers, Part III 14*. Springer, 2019, pp. 100–116.
- [36] A. Radford, J. W. Kim, C. Hallacy, A. Ramesh, G. Goh, S. Agarwal, G. Sastry, A. Askell, P. Mishkin, J. Clark *et al.*, “Learning transferable visual models from natural language supervision,” in *International conference on machine learning*. PMLR, 2021, pp. 8748–8763.
- [37] K. Simonyan and A. Zisserman, “Very deep convolutional networks for large-scale image recognition,” *arXiv preprint arXiv:1409.1556*, 2014.
- [38] A. Dosovitskiy, L. Beyer, A. Kolesnikov, D. Weissenborn, X. Zhai, T. Unterthiner, M. Dehghani, M. Minderer, G. Heigold, S. Gelly *et al.*, “An image is worth 16x16 words: Transformers for image recognition at scale,” *arXiv preprint arXiv:2010.11929*, 2020.
- [39] A. Kirillov, E. Mintun, N. Ravi, H. Mao, C. Rolland, L. Gustafson, T. Xiao, S. Whitehead, A. C. Berg, W.-Y. Lo *et al.*, “Segment anything,” *arXiv preprint arXiv:2304.02643*, 2023.
- [40] Y. LeCun, Y. Bengio, and G. Hinton, “Deep learning,” *Nature*, p. 436–444, May 2015. [Online]. Available: <http://dx.doi.org/10.1038/nature14539>
- [41] Y. Guo, Y. Liu, A. Oerlemans, S. Lao, S. Wu, and M. S. Lew, “Deep learning for visual understanding: A review,” *Neurocomputing*, vol. 187, pp. 27–48, 2016.
- [42] B. Fei, W. Yang, W.-M. Chen, Z. Li, Y. Li, T. Ma, X. Hu, and L. Ma, “Comprehensive review of deep learning-based 3d point cloud completion processing and analysis,” *IEEE Transactions on Intelligent Transportation Systems*, 2022.
- [43] W. Yuan, T. Khot, D. Held, C. Mertz, and M. Hebert, “Pcn: Point completion network,” in *2018 International Conference on 3D Vision (3DV)*. IEEE, 2018, pp. 728–737.
- [44] L. P. Tchapmi, V. Kosaraju, H. Rezatofighi, I. Reid, and S. Savarese, “Topnet: Structural point cloud decoder,” in *Proceedings of the IEEE/CVF Conference on Computer Vision and Pattern Recognition*, 2019, pp. 383–392.
- [45] M. Liu, L. Sheng, S. Yang, J. Shao, and S.-M. Hu, “Morphing and sampling network for dense point cloud completion,” in *Proceedings of the AAAI conference on artificial intelligence*, vol. 34, no. 07, 2020, pp. 11 596–11 603.
- [46] A. Vaswani, N. Shazeer, N. Parmar, J. Uszkoreit, L. Jones, A. N. Gomez, Ł. Kaiser, and I. Polosukhin, “Attention is all you need,” *Advances in neural information processing systems*, vol. 30, 2017.
- [47] M.-H. Guo, J.-X. Cai, Z.-N. Liu, T.-J. Mu, R. R. Martin, and S.-M. Hu, “Pct: Point cloud transformer,” *Computational Visual Media*, p. 187–199, Apr 2021. [Online]. Available: <http://dx.doi.org/10.1007/s41095-021-0229-5>
- [48] X. Pan, Z. Xia, S. Song, L. E. Li, and G. Huang, “3d object detection with pointformer,” in *2021 IEEE/CVF Conference on Computer Vision and Pattern Recognition (CVPR)*, Nov 2021. [Online]. Available: <http://dx.doi.org/10.1109/cvpr46437.2021.00738>
- [49] X. Yu, Y. Rao, Z. Wang, Z. Liu, J. Lu, and J. Zhou, “Pointn: Diverse point cloud completion with geometry-aware transformers,” in *Proceedings of the IEEE/CVF international conference on computer vision*, 2021, pp. 12 498–12 507.
- [50] P. Xiang, X. Wen, Y.-S. Liu, Y.-P. Cao, P. Wan, W. Zheng, and Z. Han, “Snowflakenet: Point cloud completion by snowflake point deconvolution with skip-transformer,” in *Proceedings of the IEEE/CVF international conference on computer vision*, 2021, pp. 5499–5509.
- [51] H. Zhou, Y. Cao, W. Chu, J. Zhu, T. Lu, Y. Tai, and C. Wang, “Seedformer: Patch seeds based point cloud completion with upsample transformer,” in *European Conference on Computer Vision*. Springer, 2022, pp. 416–432.
- [52] Z. Chen, F. Long, Z. Qiu, T. Yao, W. Zhou, J. Luo, and T. Mei, “Anchorformer: Point cloud completion from discriminative nodes.”
- [53] S. Li, P. Gao, X. Tan, M. Wei, and G. Pointr, “Proxyformer: Proxy alignment assisted point cloud completion with missing part sensitive transformer.”
- [54] R. Zhang, Z. Guo, W. Zhang, K. Li, X. Miao, B. Cui, Y. Qiao, P. Gao, and H. Li, “Pointclip: Point cloud understanding by clip,” *arXiv preprint arXiv:2112.02413*, 2021.
- [55] X. Zhu, R. Zhang, B. He, Z. Zeng, S. Zhang, and P. Gao, “Pointclip v2: Adapting clip for powerful 3d open-world learning,” *arXiv preprint arXiv:2211.11682*, 2022.
- [56] Y. Zeng, C. Jiang, J. Mao, J. Han, C. Ye, Q. Huang, D.-Y. Yeung, Z. Yang, X. Liang, and H. Xu, “Clip²: Contrastive language-image-point pretraining from real-world point cloud data,” *arXiv preprint arXiv:2303.12417*, 2023.
- [57] D. Hegde, J. M. J. Valanarasu, and V. M. Patel, “Clip goes 3d: Leveraging prompt tuning for language grounded 3d recognition,” *arXiv preprint arXiv:2303.11313*, 2023.
- [58] L. Xue, M. Gao, C. Xing, R. Martín-Martín, J. Wu, C. Xiong, R. Xu, J. C. Niebles, and S. Savarese, “Ulip: Learning unified representation of language, image and point cloud for 3d understanding,” *arXiv preprint arXiv:2212.05171*, 2022.
- [59] L. Xue, N. Yu, S. Zhang, J. Li, R. Martín-Martín, J. Wu, C. Xiong, R. Xu, J. C. Niebles, and S. Savarese, “Ulip-2: Towards scalable multimodal pre-training for 3d understanding,” *arXiv preprint arXiv:2305.08275*, 2023.
- [60] J. Li, D. Li, C. Xiong, and S. Hoi, “Blip: Bootstrapping language-image pre-training for unified vision-language understanding and generation.”
- [61] M. Lewis, Y. Liu, N. Goyal, M. Ghazvininejad, A. Mohamed, O. Levy, V. Stoyanov, and L. Zettlemoyer, “Bart: Denoising sequence-to-sequence pre-training for natural language generation, translation, and comprehension,” *arXiv preprint arXiv:1910.13461*, 2019.
- [62] T. Groueix, M. Fisher, V. G. Kim, B. C. Russell, and M. Aubry, “A papier-mâché approach to learning 3d surface generation,” in *Proceedings of the IEEE conference on computer vision and pattern recognition*, 2018, pp. 216–224.
- [63] Y. Yang, C. Feng, Y. Shen, and D. Tian, “Foldingnet: Point cloud auto-encoder via deep grid deformation,” in *Proceedings of the IEEE conference on computer vision and pattern recognition*, 2018, pp. 206–215.
- [64] L. Pan, “Ecg: Edge-aware point cloud completion with graph convolution,” *IEEE Robotics and Automation Letters*, vol. 5, no. 3, pp. 4392–4398, 2020.
- [65] L. Pan, X. Chen, Z. Cai, J. Zhang, H. Zhao, S. Yi, and Z. Liu, “Variational relational point completion network,” in *Proceedings of the IEEE/CVF conference on computer vision and pattern recognition*, 2021, pp. 8524–8533.
- [66] Z. Huang, Y. Yu, J. Xu, F. Ni, and X. Le, “Pf-net: Point fractal network for 3d point cloud completion,” in *Proceedings of the IEEE/CVF conference on computer vision and pattern recognition*, 2020, pp. 7662–7670.
- [67] H. Xie, H. Yao, S. Zhou, J. Mao, S. Zhang, and W. Sun, “Grnet: Gridding residual network for dense point cloud completion,” in *Computer Vision—ECCV 2020: 16th European Conference, Glasgow, UK, August 23–28, 2020, Proceedings, Part IX*. Springer, 2020, pp. 365–381.
- [68] J. Wang, Y. Cui, D. Guo, J. Li, Q. Liu, and C. Shen, “Pointattn: You only need attention for point cloud completion,” *arXiv preprint arXiv:2203.08485*, 2022.
- [69] W. Zhang, Z. Dong, J. Liu, Q. Yan, C. Xiao *et al.*, “Point cloud completion via skeleton-detail transformer,” *IEEE Transactions on Visualization and Computer Graphics*, 2022.
- [70] A. Paszke, S. Gross, F. Massa, A. Lerer, J. Bradbury, G. Chanan, T. Killeen, Z. Lin, N. Gimelshein, L. Antiga *et al.*, “Pytorch: An imperative style, high-performance deep learning library,” *Advances in neural information processing systems*, vol. 32, 2019.
- [71] D. P. Kingma and J. Ba, “Adam: A method for stochastic optimization,” *arXiv preprint arXiv:1412.6980*, 2014.